SLAC-PUB-7095
WIS-96/25/June-PH
August 1996

STUDY CsI PHOTOCATHODES : VOLUME RESISTIVITY AND AGEING

J.Va'vra*, A. Breskin, A. Buzulutskov#, R. Chechik, E. Shefer

Department of Particle Physics, Weizmann Institute of Science, Rehovot, 76100 Israel

* Visitor from Stanford Linear Accelerator Center, Stanford University, Stanford, CA 94309, U.S.A.

Presently at Budker Institute of Nuclear Physics, Novosibirsk, Russia

ABSTRACT

Wire-chamber gaseous electron multipliers coupled to CsI photocathodes, provide interesting means for UV-photon imaging over very large area. We report on the measurement of the CsI resistivity, important for the understanding of rate-dependent effects in CsI-based detectors. Photon counting at high rates is also closely connected to long-term photocathode stability. We present results on ageing of CsI photocathodes under high photon flux, with one atmosphere CH_4 and under detector gain of 10^5, for several substrate materials. We compare the ageing results with that of CsI photocathodes coated with thin NaF protective films.

Presented at the 1-st Conference on New Developments in Photodetection, Beaune, France, June 24-28, 1996.

The work was supported in part by the United States - Israel Binational Science Foundation (BSF), and Department of Energy contract DE-AC03-76SF00515.

1. INTRODUCTION

In recent years there has been a growing interest in photon detectors combining solid photocathodes and electron multipliers based on gas amplification. In particular, CsI UV-photocathodes have attracted considerable attention for applications in Ring Imaging Cherenkov (RICH) detectors [1, 2]. It has been established that the surface properties of CsI photocathode may have a strong impact on the photo-emission properties [1].

The resistive behavior of the photocathode should have an influence on the ion recombination at its surface and therefore on the rate capability of detectors based on this principle. The capability of operating at high rates is also closely related to the photocathode ageing.

The resistivity of CsI photocathodes was not studied systematically so far. There have been some works indicating that alkali halides have a volume resistivity in the range of 10^9 Ωcm at 200°C. Extrapolating to room temperature, one could expect values of 10^{10}-10^{11} Ωcm. However, the resistance of alkali halides is not quoted as a "hard constant" in the literature, and one may suspect that it is not stable. The resistivity could be influenced by the method of CsI film deposition which often determines the poly-crystalline grain size [3], heating procedure used to enhance the quantum efficiency (QE) [4], level of vacuum, exposure to air, etc.

The ageing processes of CsI photocathodes are not fully understood. It is known that the QE deteriorates due to photon impact and, under gas multiplication, due to ion impact. The principal mechanisms and a collection of existing data on CsI ageing are reviewed in [1].

Recently, there was a considerable effort to investigate the role of protective layers applied over solid photocathodes [5]. Such protective layers could be used later for the development of visible photocathodes for applications with wire chambers. Therefore, we have also included the ageing study of a CsI photocathode covered with a thin layer of NaF.

In the present article we present our results of the studies of CsI electrical resistivity in various conditions and of its ageing under photon and ion impact.

2. EXPERIMENTAL SETUP AND RESULTS

2.1. Resistivity studies

The CsI resistivity was measured using a microstrip electrode pattern deposited on a Corning glass 7740 substrate. Fig. 1 shows the strip pattern. The 1500 Å thick chromium strips were evaporated on the glass. We have selected a section of the microstrip electrode pattern having 59 gaps, each 296 μm wide, 29.3 mm long resulting in 6076 "squares". The microstrip pattern was connected to thin connection wires, using silver paint "Leitsilber 200", and secured mechanically with Varian epoxy "Torr Seal". The microstrip glass was cleaned with pure acetone and then glued to a stainless steel base, using 5 minutes Araldit epoxy, and placed into the evaporation chamber. Electrically, the stainless steel base was grounded, positive voltage was applied to the

9 μm wide strips and the 400 μm wide strips were connected to a pA-meter, according to Fig. 1. The temperature of the sample was regulated with the help of a water circulation system and a thermostatic bath. The important requirement was that the glass resistivity is large compared to the CsI resistivity.

The surface and volume resistivity are defined using Fig. 2 and the following equations :

Surface resistivity : $$\rho_s = \frac{V}{I} N_{squares} \quad (1)$$

Volume resistivity : $$\rho_v = R \frac{A}{d} = \frac{V}{I} h \frac{N_{squares}}{d}, \quad A = h N_{squares} \quad (2)$$

In the above equations, **V** is the voltage between strips (typically 100-200 V), **I** is the measured current (typically 10-5000 pA), **R** is the resulting overall resistance as defined by the Ohm law, $\mathbf{N_{squares}}$ is the number of squares in the microstrip pattern, **h** is thickness of the evaporated CsI layer (typically 30-5000 Å), **d** is the distance between strips (296 μm) and **A** is cross-sectional area of the CsI layer.

Tests with the microstrip structure, prior to CsI evaporation, were done in air and ambient temperature (22-24°C). They determined a "glass current" $\mathbf{I_g}$ of about 21±2 pA/100 V, which is equivalent to ρ_s~2.9x10^{16} Ω/square, assuming the current is a surface current. If the current propagates through the glass volume, then this calculation is not correct, and we have to specify the glass resistivity in Ωcm. However, the important point in this particular experiment is that $\mathbf{I_g}$ is small compared to the "CsI current", after the CsI evaporation on the glass surface. The value of $\mathbf{I_g}$ did not change very much when we placed the microstrip plate in the vacuum chamber. This, in fact, is suprising since one would expect a large effect due to moisture and it indicates, perhaps, that a dominant current indeed passes through the glass volume. We measured typically 20±2 pA/100 V in vacuum of ~4.7x10^{-7} Torr. The voltage dependence in vacuum is shown in Fig. 3 and indicates a good "Ohmic behavior". However, the glass was charging up and we had to wait ~15 minutes to allow for the current to stabilize. The value of $\mathbf{I_g}$ changed between 20 and 27 pA only when the glass was heated between the ambient temperature and 55°C (see Fig. 4). Nevertheless, $\mathbf{I_g}$ represented only a small correction to the CsI current under all conditions.

CsI was evaporated at vacuum of 1.2x10^{-7} Torr, and at evaporation speed of 2-20 Å/sec. The evaporation was done in steps for the following CsI layer thicknesses : 33, 110, 505, 1003, 1520, 2007, 2513, 3022, 4011 and 5008 Å. For each thickness, we measured current at three voltages : 100, 150 and 200 V. We observed an Ohmic behavior of current and voltage, for the evaporated films. Fig. 5 shows examples of typical current-voltage dependence for various thicknesses of CsI. For the 33 Å thickness, the measured current was essentially the same as that of the glass,

indicating that the CsI layer is not yet continuous. The measured current (at 100 V) is increasing linearly with the CsI thickness - see Fig. 6. This indicates that the electrical current goes through the CsI volume rather than along its surface. Therefore, we quote CsI resistivity as volume resistivity. The average volume resistivity of a "fresh" CsI layer, which was not subject to any heat treatment or air exposure, is ~$1.2 \times 10^{10}\,\Omega$cm at ambient temperature and vacuum of ~1×10^{-7} Torr. Such "fresh" photocathode has still a poor quantum efficiency and it must be enhanced by a heat treatment [4].

To study the effect of the heat treatment on the CsI resistivity we cycled the temperature six times over a period of ~150 hours. Each thermal cycle changed temperature between ~3°C and ~80°C in 10-20°C steps. We kept 100 V across the microstrip electrodes during the entire test. Fig. 7 shows that the volume resistivity increased by a factor of 10 during the test. It is not clear what caused the volume resistivity increase. It could be the effect of (a) thermal cycling, (b) prolonged vacuum effect acting on the water content inside the CsI layer, (c) the presence of a current in the CsI layer throughout the entire experiment. We have tried to investigate each variable separately :

(a). During each thermal cycle we determined the volume resistivity corresponding to 23°C. The plot of these values is shown in Fig. 8 (closed circles). After ~150 hours, we stopped the thermal cycling and continued with pumping only (open circles in Fig. 8), while keeping a vacuum of 5-7x10^{-8} Torr. Fig. 8 shows that the volume resistivity increased to ~$1.2 \times 10^{11}\,\Omega$cm at 23°C even without the thermal cycling.

(b) We deteriorated the vacuum down to 5-6x10^{-5} Torr for about 8 hours. Fig. 9 shows that the corresponding volume resistivity decreased to ~$7 \times 10^{10}\,\Omega$cm within one hour. The vacuum was then restored to 3-4x10^{-8} Torr. Although the volume resistivity started to increase again, it did not reach the previous value of $1.2 \times 10^{11}\,\Omega$cm, even after ~15 hours under high vacuum - see Fig. 9. The most interesting part of this test occurred when we introduced air into the chamber for about 10 minutes (+8°C Dewpoint, i.e. 42.9% relative humidity). This procedure was chosen to simulate exposure to air during the transfer of a photocathode to a detector. The current increased from 345 pA to 1.1 μA (at 100 V), corresponding to a volume resistivity ~$2.8 \times 10^{7}\,\Omega$cm. As soon as we started pumping again, the current decreased rapidly. Already at a vacuum of 6x10^{-5} Torr, we measured ~50 pA/100 V, which is comparable to the current measured with the glass substrate - see Fig. 3. The corresponding volume resistivity was ~$6 \times 10^{11}\,\Omega$cm.

It was published earlier [3] that evaporated CsI layers, after a short exposure to air, consist of small grains, typically ~1 μm in size. In the present setup the grain size and the modification of its boundary, could strongly affect the resistivity across the distance between strips. On the contrary, in a typical Fast Ring Imaging Cherenkov detector with a pad

electrode structure, the electric field is orthogonal to that in our test, and the CsI grain structure may actually help to increase conductivity. On the other hand, during normal pumping or a long term gas flowing, the CsI resistivity may be modulated primarily by the moisture content.

(c) The nature of the current between the microstrip electrodes is another subject to consider. Generally, the current in alkali halides is of an ionic origin [6]. It is caused by the crystal impurities which allow for a charge transfer throughout the crystal. In a perfect crystal, there should be a very small electrical conduction. The ionic nature of the current was proved experimentally by observing ionic deposits on the electrodes in amounts proportional to the total accumulated charge. It is very similar to the electrolysis in liquids. This means that I^- ions will actually migrate to the anode and Cs^+ ions to the cathode, where they will either deposit as atoms or react with the chromium metal of the strips. It is interesting to note that iodine is very resistive (~1.3×10^9 Ωcm), whereas cesium is a good conductor (~$2 \times 10^{-5} \Omega$cm). Therefore, the excessive iodine build up on the anode strips would increase the resistivity. We estimate about 8 iodine ions deposited per area of about 10x10 $(\text{Å})^2$ of the anode strip, in ~5 days of running, which doesn't appear as a significant amount.

The photocathode quantum efficiency (QE) was also measured periodically during the resistivity measurements. In this case all the strips on the glass substrate were interconnected and read out by a pA-meter; an 81% transparent stainless steel grid, placed at about 2.5 mm above the CsI layer, was connected to a voltage source, set to 400 V, to create a photoelectron extraction gradient of about 1 kV/cm. The QE of CsI on the microstrip substrate was essentially the same as the one measured usually on a continuous metal substrate.

Very first QE values, measured immediately after the evaporation, were poor, as observed in Ref. 5. However, after a few hours of heating at 55°C they enhanced to the usual good values - see Fig. 10. Fig. 11 shows that the substrate temperature during the QE measurement did not significantly affect the result. Fig. 12 shows the QE values measured at 23°C during the heating cycles (Fig.7). Over this period the volume resistivity changed by more than a factor of ~10, but we do not see a significant variation in the QE. However, after the microstrip structure was exposed to air for only ~10 minutes, the QE was affected significantly - see Fig. 13. This result contradicts previous observations that a "heat-enhanced" photocathode is stable for more than 30 min while exposed to air [4]. It could be due to the fact that this particular sample has been previously subject to various other tests.

We discovered that on the edges of the wide strips (anodes in this setup) a white deposit was clearly seen after only a week of running under 100 V across the strip structure. The deposits extended over about 10% of the strip width. As discussed above, the anode strips are subject to the iodine electrolytic plating. The CsI layer could be simply cleaned by repeated rinsing in de-

ionized water and ethanol. No sign of a discoloration was observed which would indicate a chemical reaction of the iodine and the chromium.

2.2. Discussion of the CsI resistivity results in terms of high rate applications

We consider a film with a volume resistivity ρ_v and a relative dielectric constant ε_r, which is deposited on a cathode plane. To estimate the maximum rate capability, we will consider the time domain only. The absolute gain is also important, but we neglect it in the present analysis.

The time constant related to the neutralization of the ionic charge is RC ~ $\varepsilon_r . \varepsilon_o . \rho_v$. Let us assume that we repeat the charge deposition on a spot comparable to the avalanche size with a mean time interval T, corresponding to a rate r = 1/T. To prevent a charge build up on the film surface, the discharge time constant, RC, should be much smaller than T: RC < 0.1 T. Therefore the maximum rate before observing charge up problems is r_{max} ~ 1/(10 RC) = 1/(10 $\varepsilon_r . \varepsilon_o . \rho_v$). If we take, for example, ε_r~4, ε_o=8.87 pF/m, and ρ_v~2.8x10^7 Ωcm, corresponding to our lowest CsI volume resistivity when exposed to air, the maximum rate capability for events occurring at a single spot is r_{max} ~10 kHz. However, a volume resistivity increase by five orders of magnitude may reduce the maximum rate capability to about 1 Hz. In real situations the individual avalanches occur at different locations. This will, of course, result in an overall improvement of the rate handling capability. Using the input from this paper, one may have to use a Monte Carlo method to evaluate quantitatively the effect in any specific detector.

2.3. Ageing studies

The experimental setup for the ageing study is shown in Fig. 14. The detector under investigation was a wire chamber with 2 mm anode-to-cathode distance, 2 mm wire pitch and 20 μm in diameter gold plated tungsten anode wires. The photocathode material was evaporated in a separate evaporation vessel (used for the QE and resistivity measurements discussed previously). The photocathode material under study was either CsI, or CsI coated with a thin layer of NaF, about 18 Å thick. Various substrate materials were used : a polished stainless steel plate, a copper-clad printed circuit board (PCB) covered with Sn/Pb alloy [7], and a copper-clad PCB chemically covered with Ni and Au [2, 8, 9]. In all cases the evaporation chamber was vented with dry nitrogen and then the photocathode was briefly exposed to air during the transfer to the ageing vessel. The transfer would typically last a few minutes, followed immediately by pumping (the ageing setup was backed by a turbo pump with a mechanical pump equipped with an oil filter). We typically reached a vacuum of 1-2x10^{-4} Torr before letting the gas enter the ageing vessel. The chamber was operating in flow mode with CH_4, of 99.995% purity. The oxygen level was typically ~5 ppm downstream of the test vessel. The oxygen level, gas pressure and temperature variations were monitored during the test. Among materials used for

construction of the detector and its vessel we should mention those which may influence the results : copper gas tubing, Viton O-rings, vacuum grease, G-10, Nylon, 5 minutes Araldit epoxy.

The photocurrent was induced by an Ar(Hg) UV light source, using its 185 nm wavelength component, as was demonstrated by attenuation of the photocurrent when placing an Aclar foil into the UV photon flux (Aclar does not transmit below ~200 nm). The irradiated surface was ~103.5 mm^2, and a typical photocurrent of a "fresh" photocathode was 5-10 nA collected from both the photocathode and the grid - see Fig.14. The lamp stability was monitored using a Hamamatsu S1337-10108Q photo-diode. The light flux was adjusted with Oriel metallic ND filters.

In the first ageing test we have studied the photocathode deterioration under photon flux only, i.e. the MWPC chamber was operating with no charge multiplication. We used a 500 nm CsI layer on a polished stainless steel substrate. The initial photocurrent density was about ~0.3 nA/mm^2 and the incident photon flux ~1.2×10^{10} photons/mm^2 per sec (the photon flux was estimated assuming QE = ~0.16 at 185 nm - see Fig. 10). Fig. 15 shows the relative photocurrent change as a function of accumulated charge dose, and indicates a 20% loss after ~20 $\mu C/mm^2$.

Next, we have measured the MWPC gain curve, recording the current of the detector as a function of the voltage - see Fig.16. During the gain measurement we were careful to check that we do not observe any self-sustaining cathode current, known as the Malter effect. This was done by a periodic interruption of the UV light and checking that the measured current is consistent with the chamber dark current, of ~0.2 nA.

In the photocathode ageing test we chose to operate the MWPC at a total gain of 10^5. The ND filters were adjusted so that the starting photocurrent density was ~0.027 nA/mm^2 and the incident photon flux ~1×10^4 photons/mm^2 per sec. We used a 500 nm CsI layer on a polished stainless steel substrate. Fig. 17 shows the relative photocurrent change as a function of charge dose, and indicates a 20% loss after ~1 $\mu C/mm^2$. This is a much faster deterioration than in the previous test with no gas gain, indicating that the mechanisms involving positive ion impact on the photocathode may be very important for the ageing process. A more detailed discussion on the ageing mechanisms is given in ref. 1.

The damaged photocathode was removed from the ageing vessel and placed again in the evaporation vessel where we re-measured the quantum efficiency (the exposure to air was less than 2-3 minutes and dry nitrogen was used for venting, in all cases). Fig. 18 shows that the photocathode QE is lower by ~30% at 185 nm compared to the initial one, i.e. the photocurrent loss is likely due to a degradation of the photocathode (QE loss) and less likely due to a degradation of the MWPC (anode wire coating).

Next, we measured the ageing of a CsI layer, evaporated on stainless steel substrate and coated with a thin film of NaF, of about 18 Å thick. We have reached a similar maximum gain and no Malter effect was observed - see Fig.16. The ageing test was performed at a total gas gain of 10^5. The total dark current at this gain was, again, negligible ~0.2nA. The ND filters were adjusted so that the starting photocurrent density was ~0.016 nA/mm^2 and the incident photon flux ~1x10^4 photons/mm^2 per sec. Fig. 19 shows the relative photocurrent change as a function of charge dose, and indicates a 20% loss after ~0.8 μC/mm^2. The degraded photocathode was removed from the ageing vessel and placed in the evaporation vessel, where we measured a relative QE loss of ~45% at 185 nm.

Next, we measured the ageing of a CsI layer deposited on two different substrates, currently used in RICH detector prototypes. Fig. 20 shows the ageing result of a 500 nm CsI evaporated on a copper-clad PCB covered with Sn/Pb alloy [7]. We observe an initial photocurrent decrease of ~25% after ~3 μC/mm^2, followed by a sudden rise and then a gradual decrease to ~25% loss after ~10 μC/mm^2. The test was terminated at this point.

Fig. 21 shows the ageing result of a 1000 nm CsI evaporated on a copper-clad PCB chemically covered with Ni and Au [2, 8, 9]. We have observed a similar erratic photocurrent behavior. Initially, the photocurrent decreased by ~10% after ~10 μC/mm^2, followed by a sudden rise to ~145% of the initial value, and then decreasing by ~25% after ~90 μC/mm^2. For both samples, the absolute QE was measured before and after the ageing test. The results were consistent with the relative drop of the photocurrent at the end of the test.

Our ageing results under charge multiplication can be compared to recent published results. A 20% loss was observed by C. Lu et.al. [10] after a charge dose ~15 μC/mm^2 at low gas pressure and a total gas gain of ~10^5, and by Krizan et.al. [11] after ~80μC/mm^2 at normal pressure and a total gas gain of ~10^5.

Clearly, there are many variables influencing the ageing process, which are not understood presently. For example, as discussed in the previous chapter, the I^- and Cs^+ ions will migrate to their respective electrode, the ionic migration being triggered by the photocurrent. The Cs^+ ions will migrate to the top of the CsI layer, in our MWPC detector geometry, and may react strongly with oxygen or other impurities present in the gas. Extremely high purity may be essential. Similarly, the role of the substrate in the ageing process is not understood.

CONCLUSIONS

We conclude that the CsI resistivity may not be a stable quantity and may be influenced by various experimental conditions. For example, we measured ρ_v~1.2x10$^{10}\Omega$cm just after the evaporation, ~1.2x10$^{11}\Omega$cm after one week of pumping and maintaining a good vacuum, ~3x10$^7\Omega$cm during a 10 minute exposure to air, and ~6x10$^{11}\Omega$cm a few hours later, while

pumping again and restoring a good vacuum. In a typical application which would start with air exposure and then would continue by flowing a pure gas for several years, one may observe large changes in resistivity, perhaps of several orders of magnitude. In applications where a large ion density is contemplated, the CsI resistivity can easily be a limiting factor in the detector operation.

After only one week of maintaining 100 V across the anode-cathode micro-strip structure, covered by the CsI photocathode, plating deposits were clearly seen on the anode electrode, after it was subsequently exposed to air. The deposits are believed to be iodine, because the ions migrate under the influence of the potential in alkali halides.

We have not found a correlation between the CsI quantum efficiency and the layer volume resistivity over the range of conditions defined in our experimental setup.

The ageing of CsI photocathode on a stainless steel substrate, with photon flux only, (no gas gain) resulted in a 20% photocurrent loss after a charge dose ~20 $\mu C/mm^2$.

Both CsI and CsI+NaF photocathode show normal gain behavior under gas multiplication. No sign of charging effects or self-sustaining cathode current was observed.

The CsI photocathode ageing in a MWPC chamber, operating with 1 atm CH_4 at a total gas gain ~10^5, resulted in a 20% photocurrent loss after : (i) a charge dose of only ~1 $\mu C/mm^2$ using a stainless steel substrate and limiting the total accumulated charge dose to only ~3 $\mu C/mm^2$, (ii) a charge dose of ~6-8 $\mu C/mm^2$ using a copper-clad PCB covered with the Sn/Pb alloy [7], and limiting the total accumulated charge dose to only ~10 $\mu C/mm^2$, and (iii) a charge dose of ~90 $\mu C/mm^2$ using a copper-clad PCB chemically covered with Ni and Au [2, 8, 9], and limiting the total accumulated charge dose to only ~100 $\mu C/mm^2$.

The CsI+NaF photocathode ageing in a MWPC chamber operating with 1 atm CH_4 at a total gas gain ~10^5 resulted in a 20% photocurrent loss after a charge dose of only ~0.8 $\mu C/mm^2$, using a stainless steel substrate and limiting the total accumulated charge dose to only ~1 $\mu C/mm^2$. In all cases the relative loss of photocurrent was consistent with absolute QE measurements.

The large differences between ageing results of CsI layers evaporated on different substrate materials may indicate the important role of the substrate in this process. The influence of the substrate material on the grain structure, the QE and the stability of the photocathode was already discussed [1, 2, 9]. However, the fact that only a single sample of each type was studied does not permit any serious discussion at this point. More measurements are needed in order to understand the ageing processes of various solid photocathode materials. These measurements should include a larger number of samples and extend the total accumulated charge dose to at least ~100 $\mu C/mm^2$.

ACKNOWLEDGMENTS

One of us (J.V.) would like to thank the Weizmann group for the excellent working conditions during his stay at the Weizmann Institute in 1995, which made these measurements possible.

FIGURE CAPTIONS

1. A schematic description of the resistivity measurement setup: the solid photocathodes, such as CsI, is evaporated on a micro-strip structure made on Corning glass 7740 substrate.
2. Details of the strip structure on the Corning glass 7740 substrate.
3. The current-voltage dependence of the glass substrate, indicating a good "Ohmic behavior" in vacuum; the current is negligible compared to the CsI current.
4. The current-temperature dependence of the glass substrate, indicating a sufficiently small leakage current even at 60°C.
5. The current-voltage dependence for various CsI thicknesses, indicating a good "Ohmic behavior"; CsI thicknesses are 110 Å (open squares), 505 Å (open circles), 1003 Å (closed circles) and 1520 Å (open triangles).
6. The measured current between strips as a function of CsI thickness at 100 V. The linear increase with the CsI thickness indicates that the electrical current propagates through the CsI volume rather than along its surface.
7. The CsI volume resistivity as a function of temperature, for several heating/cooling cycles. The resistivity changed by a factor of more than 10, compared to a "fresh" CsI sample, during the heat cycling and the prolonged pumping period of ~150 hours.
8. Volume resistivity as a function of time. For each thermal cycle of Fig. 7, we determined the volume resistivity corresponding to 23°C (closed circles). After ~150 hours, we stopped the thermal cycling and continued measurements under high vacuum of $5\text{-}7 \times 10^{-8}$ Torr (open circles).
9. The dependence of the (a) current per 100 V across the micro-strip structure, and (b) volume resistivity of the CsI photocathode on the quality of vacuum and exposure to air.
10. The quantum efficiency as a function of wavelength for the freshly evaporated CsI photocathode, and after 2-4 hours heating period at 55°C; this photocathode was subsequently used during he resistivity measurements - see the first two points of Fig. 7.
11. The CsI quantum efficiency as a function of wavelength and the photocathode temperature.
12. A comparison of the CsI quantum efficiency before, during and after the heat cycling, as described in Fig. 7, corresponding to a volume resistivity changed by more than a factor of 10.
13. The QE of the CsI photocathode subject to the heat cycle, prior and after a 10 min exposure to air; a relatively small effect on the QE was observed; the volume resistivity changed by a factor of 6 after the vacuum was restored - see Fig.9.

14. The experimental setup used to study ageing of solid photocathodes.
15. The CsI photocathode ageing induced by light flux only (chamber had no gain) with CH_4 gas at 1 atm. 500 nm CsI on polished stainless steel (ss) substrate.
16. Total gas gain dependence on voltage in the MWPC chamber operating with CH_4 at 1 atm, and equipped with a stainless steel (ss) substrate and the following coatings: (a) a 500 nm of CsI (open circles), and (b) a 500 nm of CsI, coated with ~18 Å of NaF (closed circles).
17. The CsI photocathode ageing induced by gas gain and light flux, with CH_4 at 1 atm at a gain of 10^5. 500 nm CsI on polished ss substrate.
18. The quantum efficiency as a function of wavelength, measured before and at the end of the CsI photocathode ageing test of Fig. 17.
19. The CsI+NaF photocathode ageing induced by gas gain and light flux with CH_4 at 1 atm and gain of 10^5. 500 nm CsI+18 Å NaF, on a stainless steel (ss) substrate.
20. The CsI photocathode ageing induced by gas gain and light flux with CH_4 at 1 atm and gain of 10^5. 500 nm CsI was evaporated on a copper-clad PCB covered with Sn/Pb alloy [7].
21. The CsI photocathode ageing induced by gas gain and light flux with CH_4 at 1 atm and gain of 10^5. 1000 nm CsI was evaporated on a copper-clad PCB chemically covered with Ni and Au [2, 8, 9].

REFERENCES

1. A.Breskin, Nucl.Instr.&Meth., A371(1996)116.
2. F. Piuz, Nucl.Instr.&Meth., A371(1996)96.
3. J. Almeida et.al., Nucl.Instr.&Meth., A367(1995)337.
4. A. Buzulutskov, A. Breskin and R. Chechik, Nucl.Instr.&Meth., A366(1995)410.
5. A. Buzulutskov, A. Breskin, R. Chechik and J. Va'vra, Nucl.Instr.&Meth., A371(1996)147.
6. N.W. Ashcroft, N.D. Mermin, Solid State Physics, p. 621, N.Y., Holt, Rinehart and Winston, 1976.
7. The substrate was provided by P. Krizan.
8. The substrate was provided by F. Piuz (PC24 substrate).
9. A. Bream et.al., Nucl.Instr.&Meth., A343(1994)163.
10. C. Lu et.al., Nucl.Instr.&Meth., A371(1996)155.
11. P. Krizan et.al., IJS report, IJS-DP-7087, October 1994.

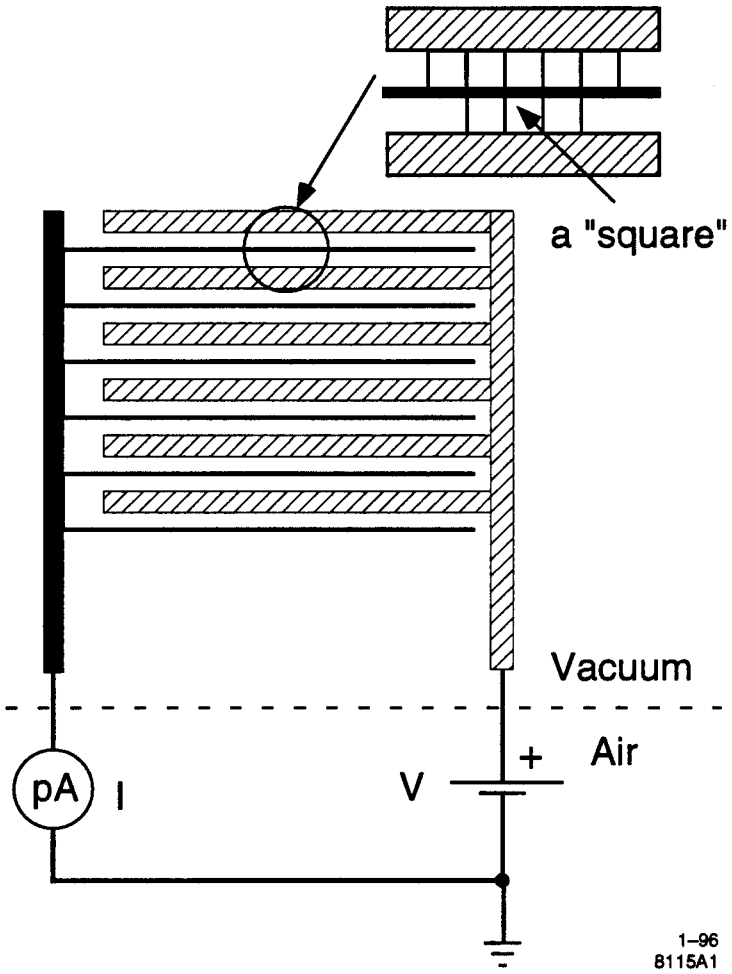

Fig. 1

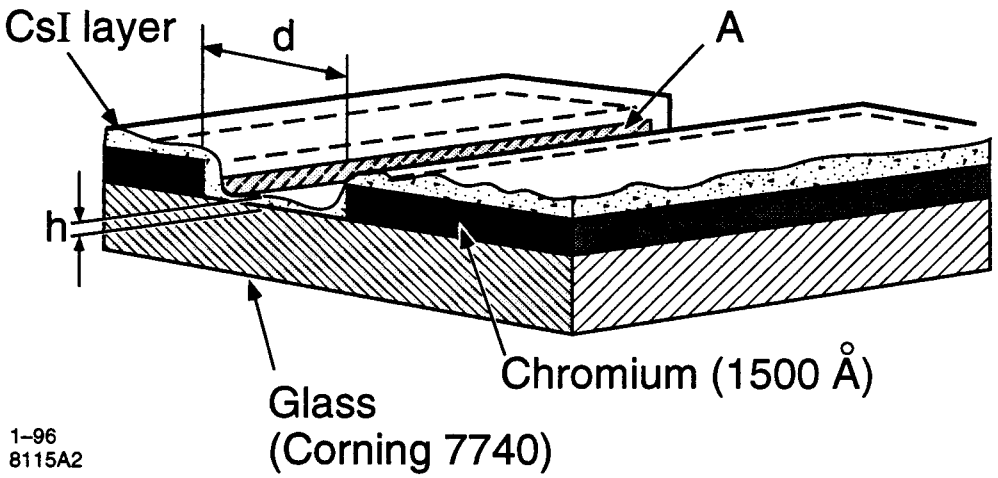

Fig. 2

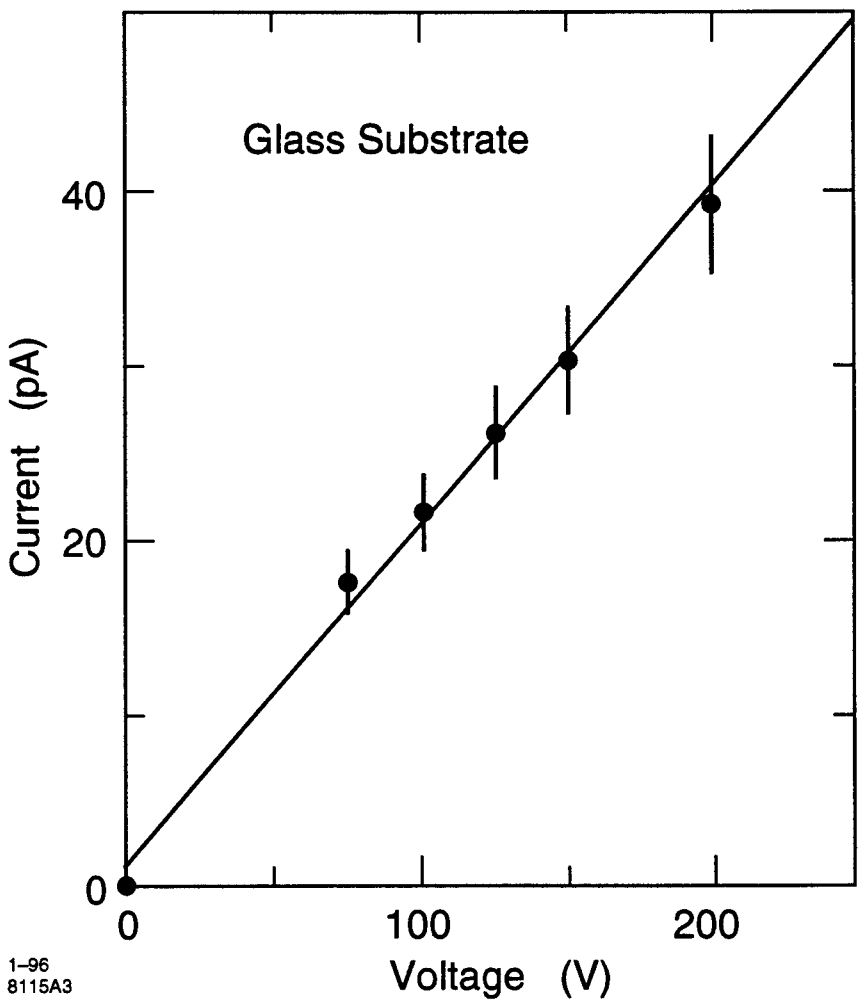
Glass Substrate
40
20
0
Current (pA)
0
100
200
Voltage (V)
1-96
8115A3

Fig. 3

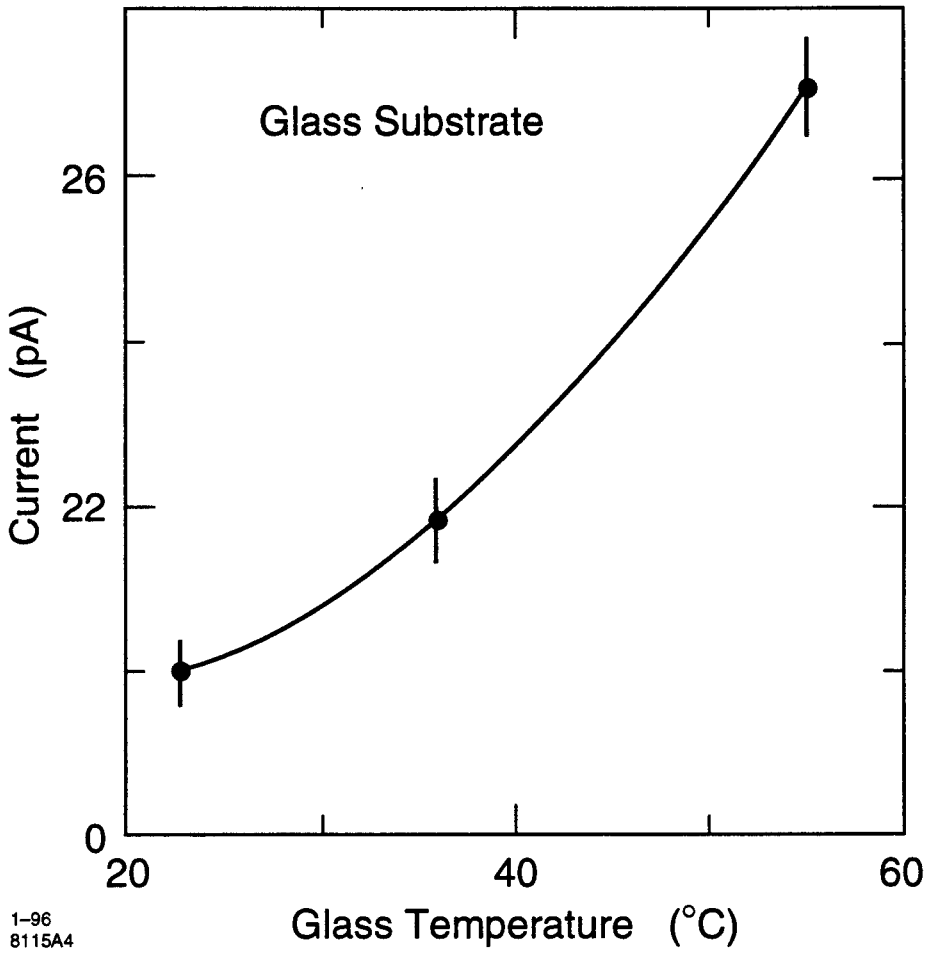
Glass Substrate
26
22
0
Current (pA)
20
40
60
Glass Temperature (°C)
1-96
8115A4

Fig. 4

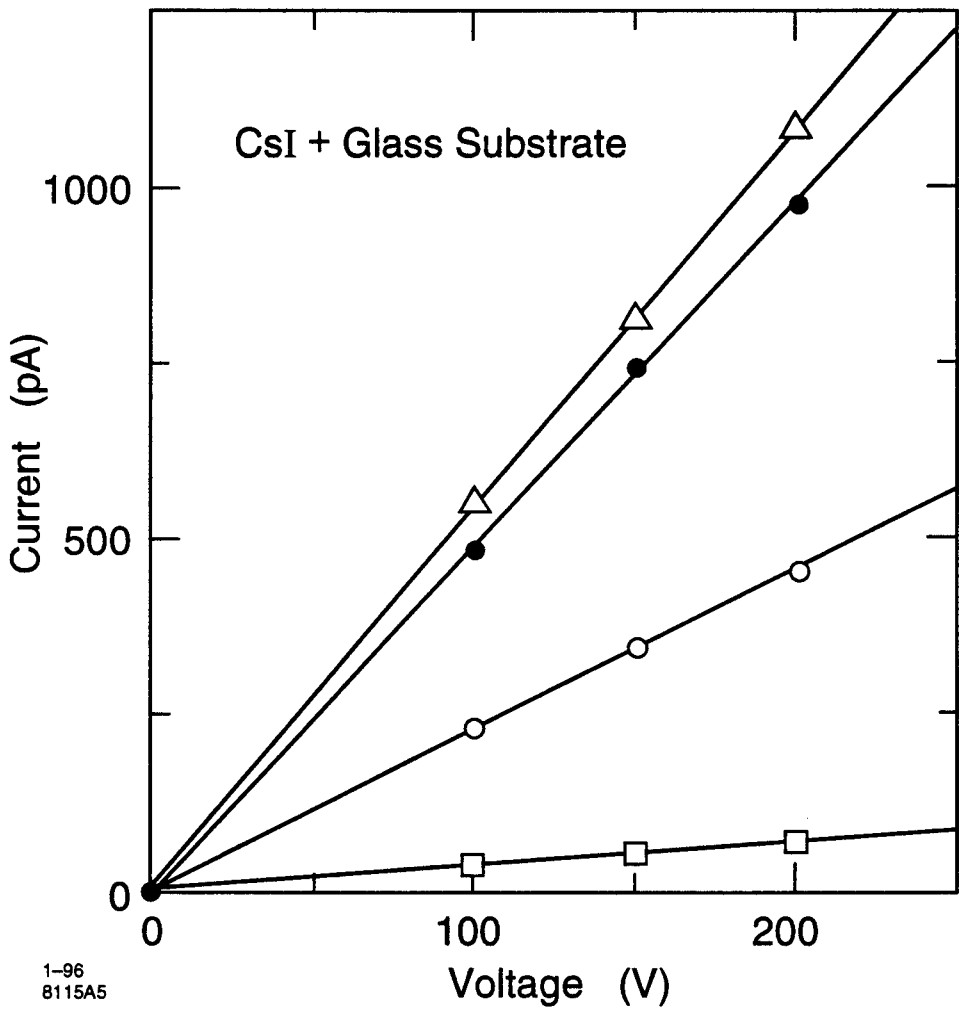
CsI + Glass Substrate
1000
500
0
Current (pA)
0
100
200
Voltage (V)
1-96
8115A5

Fig. 5

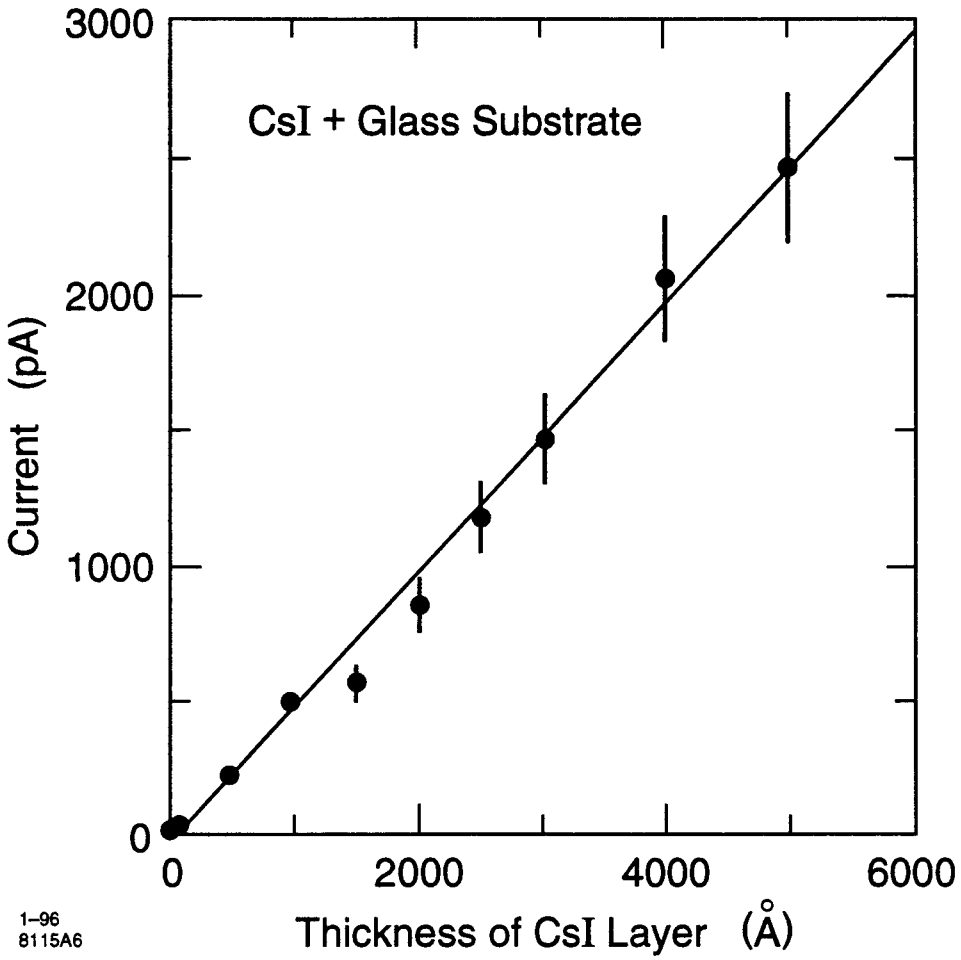
3000
2000
1000
0
CsI + Glass Substrate
Current (pA)
0
2000
4000
6000
Thickness of CsI Layer (Å)
1–96
8115A6

Fig. 6

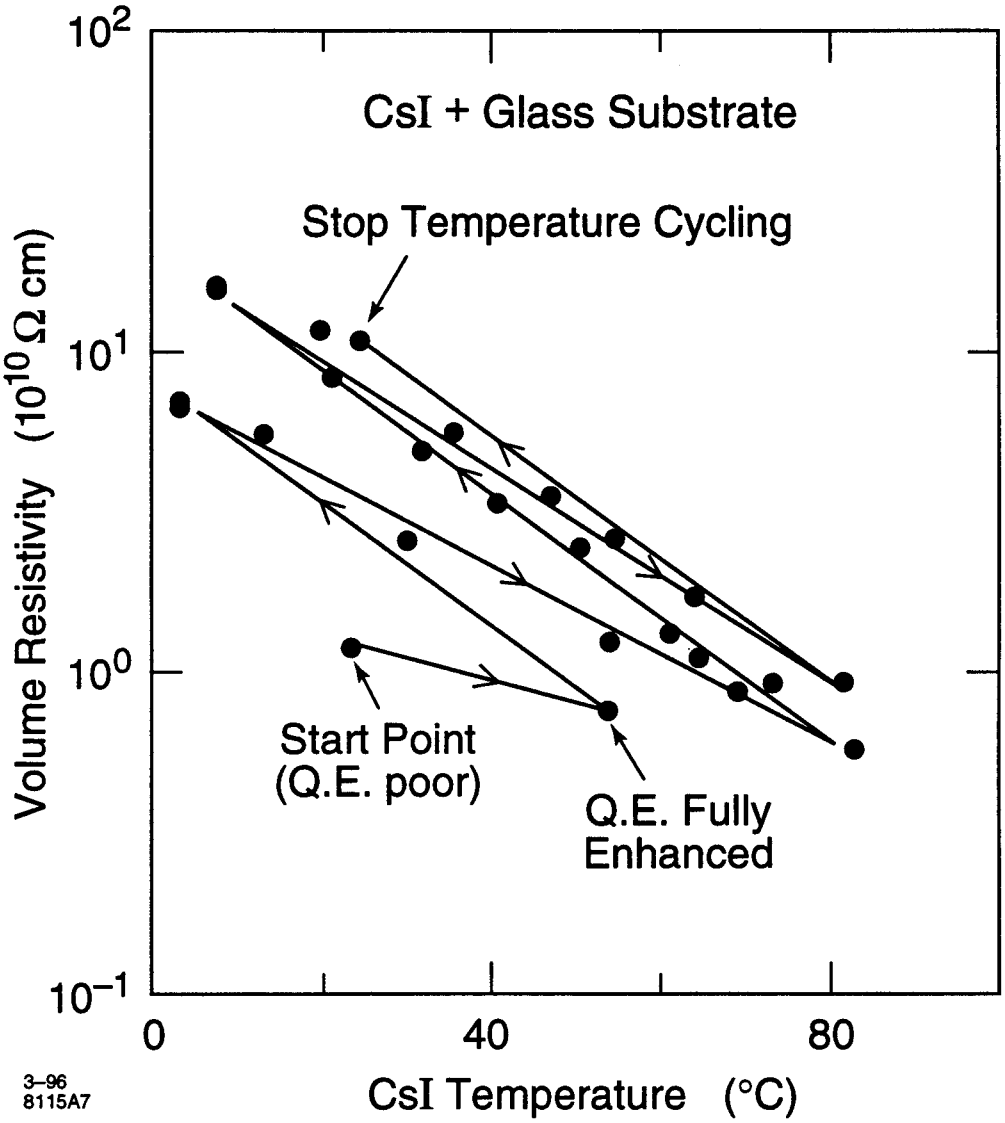
CsI + Glass Substrate
Stop Temperature Cycling
Start Point
(Q.E. poor)
Q.E. Fully
Enhanced
Volume Resistivity ($10^{10}\Omega$ cm)
10^2
10^1
10^0
10^{-1}
0
40
80
CsI Temperature (°C)
3-96
8115A7

Fig. 7

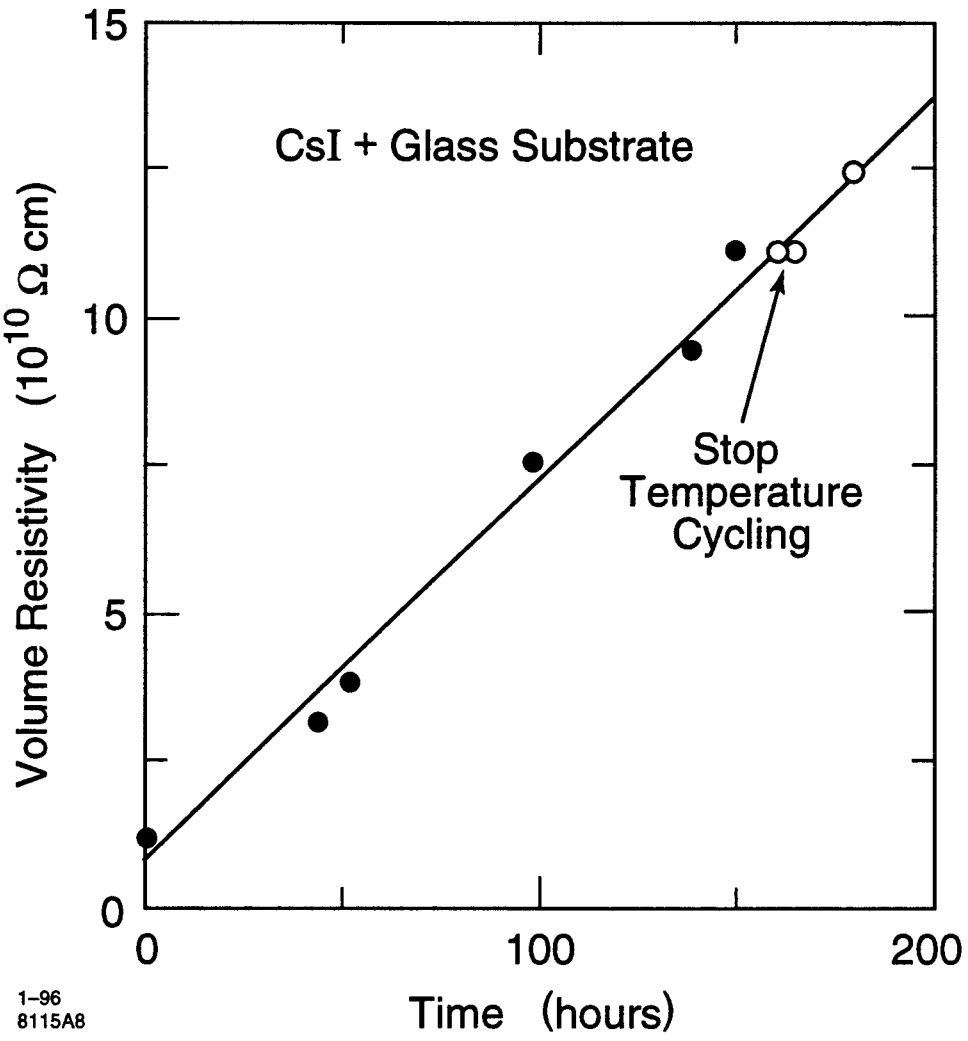
15
10
5
0
0
100
200
CsI + Glass Substrate
Stop
Temperature
Cycling
Volume Resistivity (10^10 Ω cm)
Time (hours)
1-96
8115A8

Fig. 8

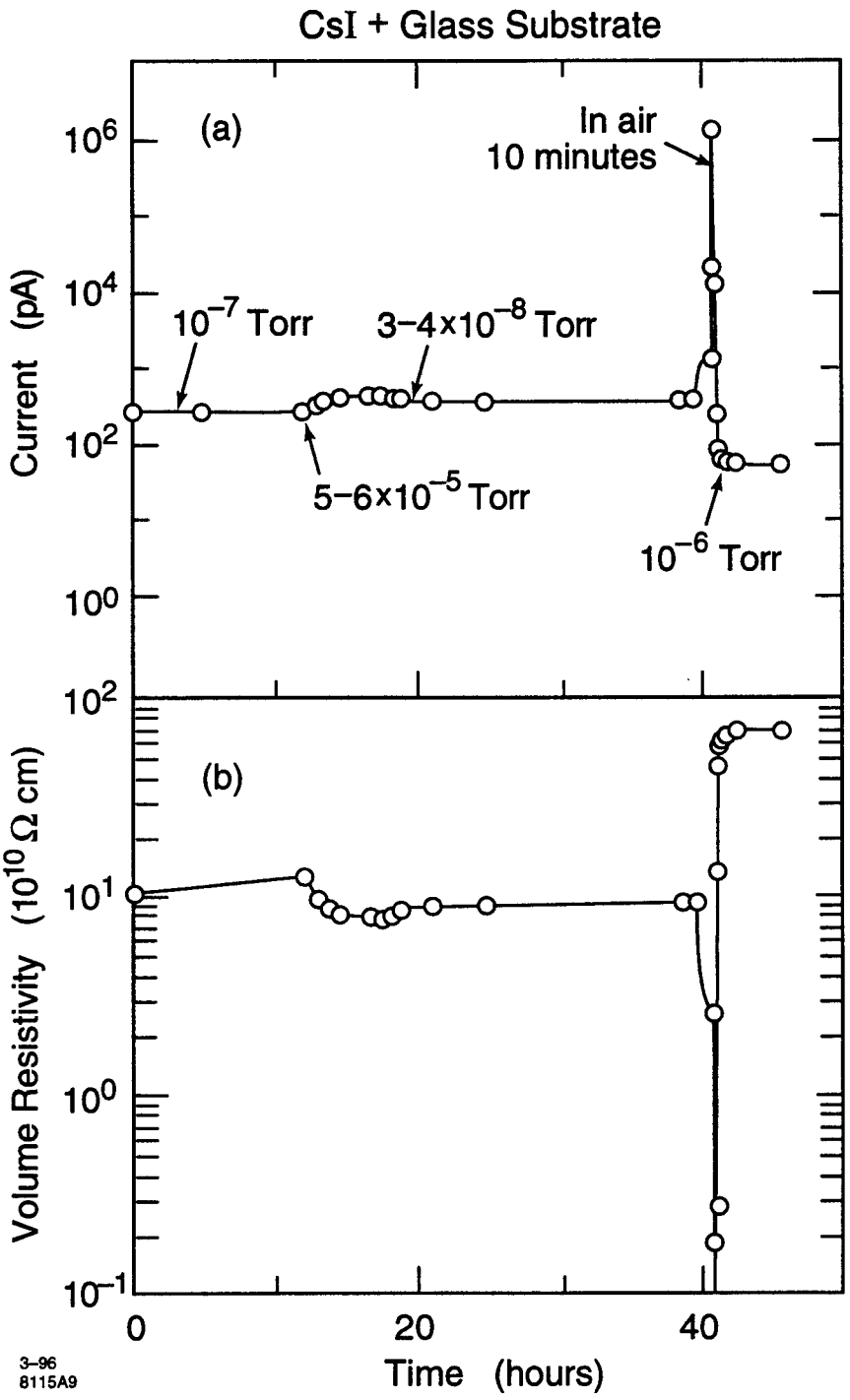
CsI + Glass Substrate
(a)
In air
10 minutes
10^{-7} Torr
3–4x10^{-8} Torr
5–6x10^{-5} Torr
10^{-6} Torr
Current (pA)
10^6
10^4
10^2
10^0
(b)
Volume Resistivity (10^{10} Ω cm)
10^2
10^1
10^0
10^{-1}
0
20
40
Time (hours)
3–96
8115A9

Fig. 9

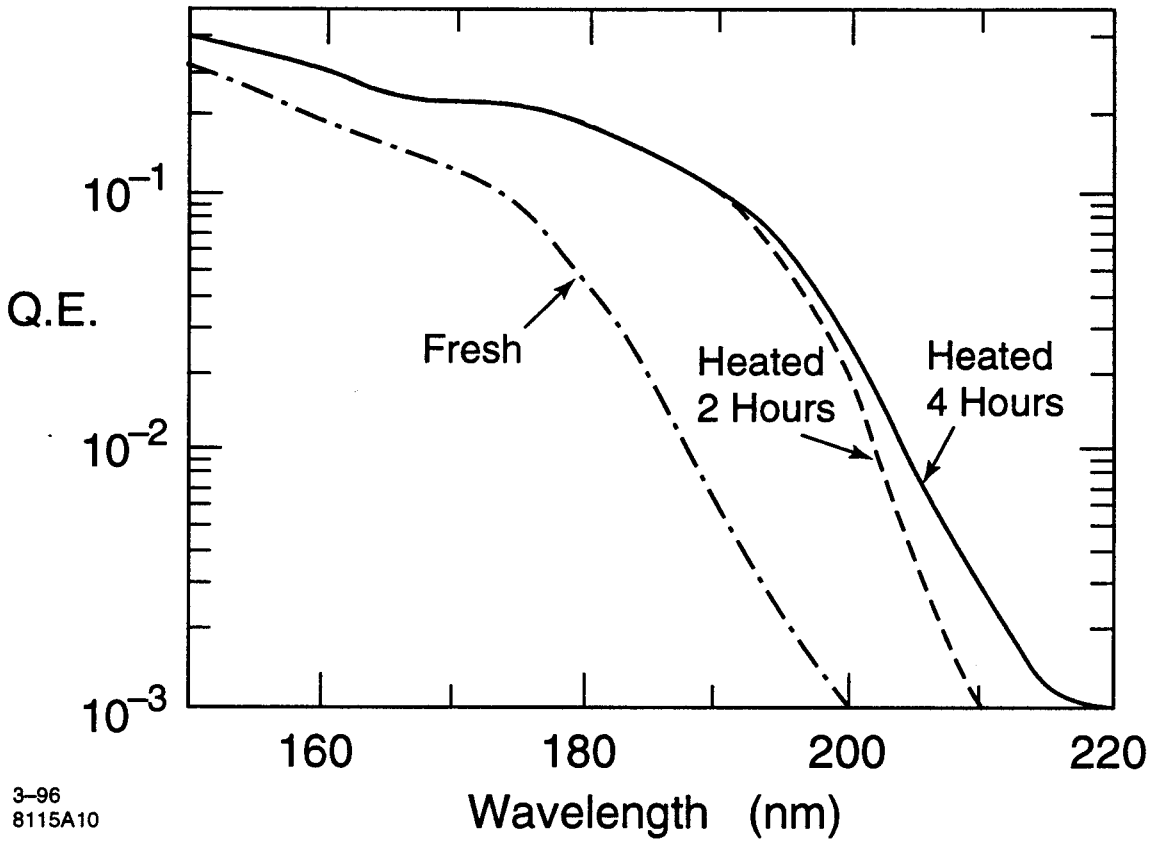
Q.E.
10^{-1}
10^{-2}
10^{-3}
Fresh
Heated
2 Hours
Heated
4 Hours
160
180
200
220
Wavelength (nm)
3–96
8115A10

Fig. 10

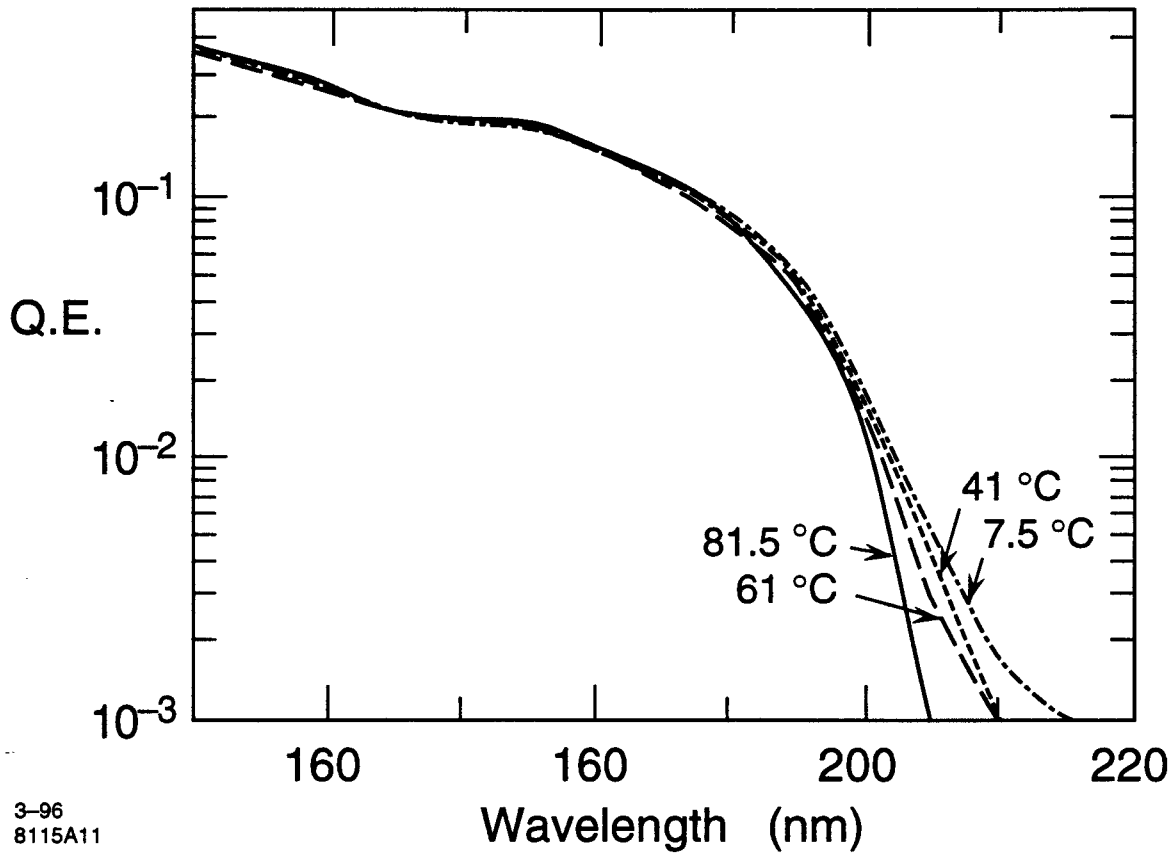
Q.E.
10^{-1}
10^{-2}
10^{-3}
41 °C
7.5 °C
81.5 °C
61 °C
160
160
200
220
Wavelength (nm)
3–96
8115A11

Fig. 11

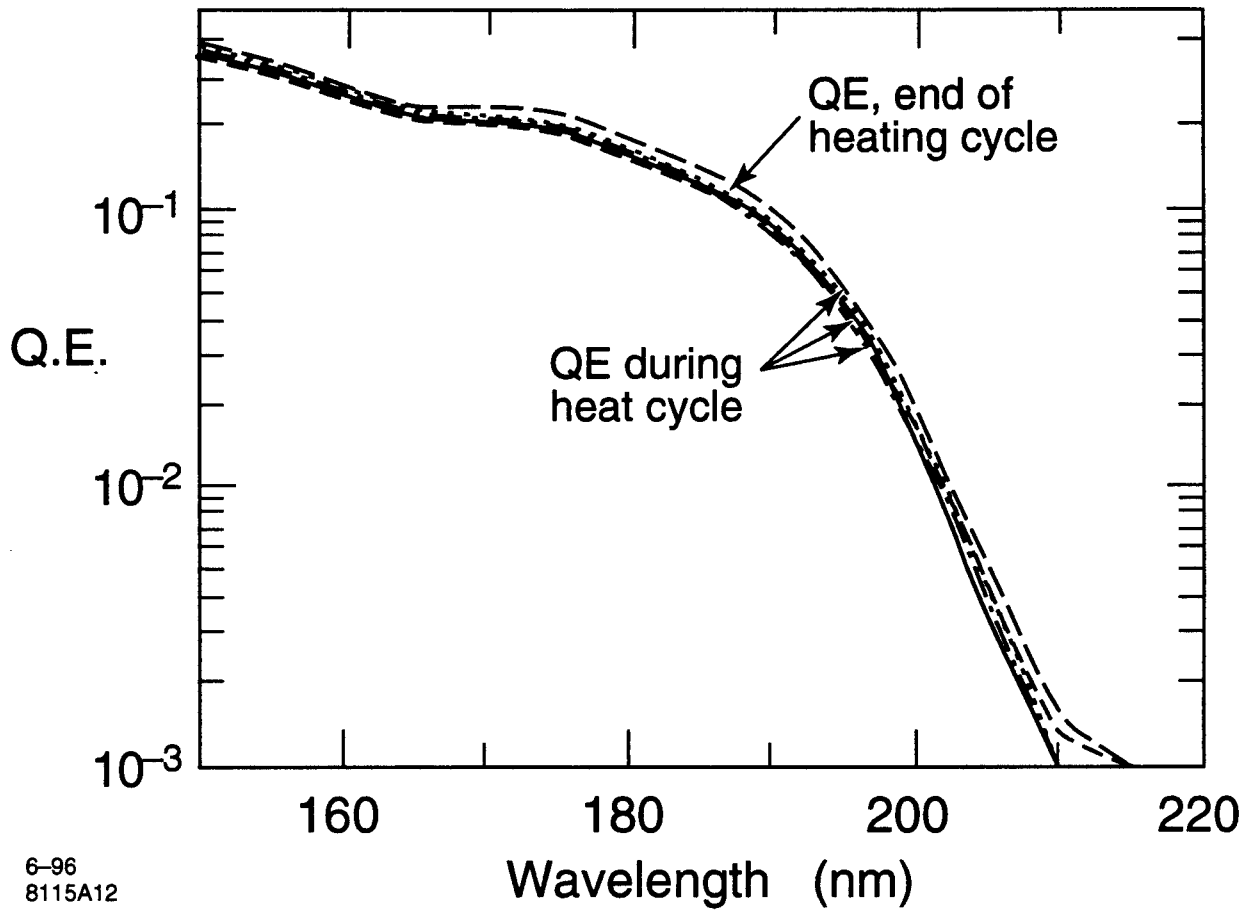
QE, end of
heating cycle
QE during
heat cycle
Q.E.
10^{-1}
10^{-2}
10^{-3}
160
180
200
220
Wavelength (nm)
6-96
8115A12

Fig. 12

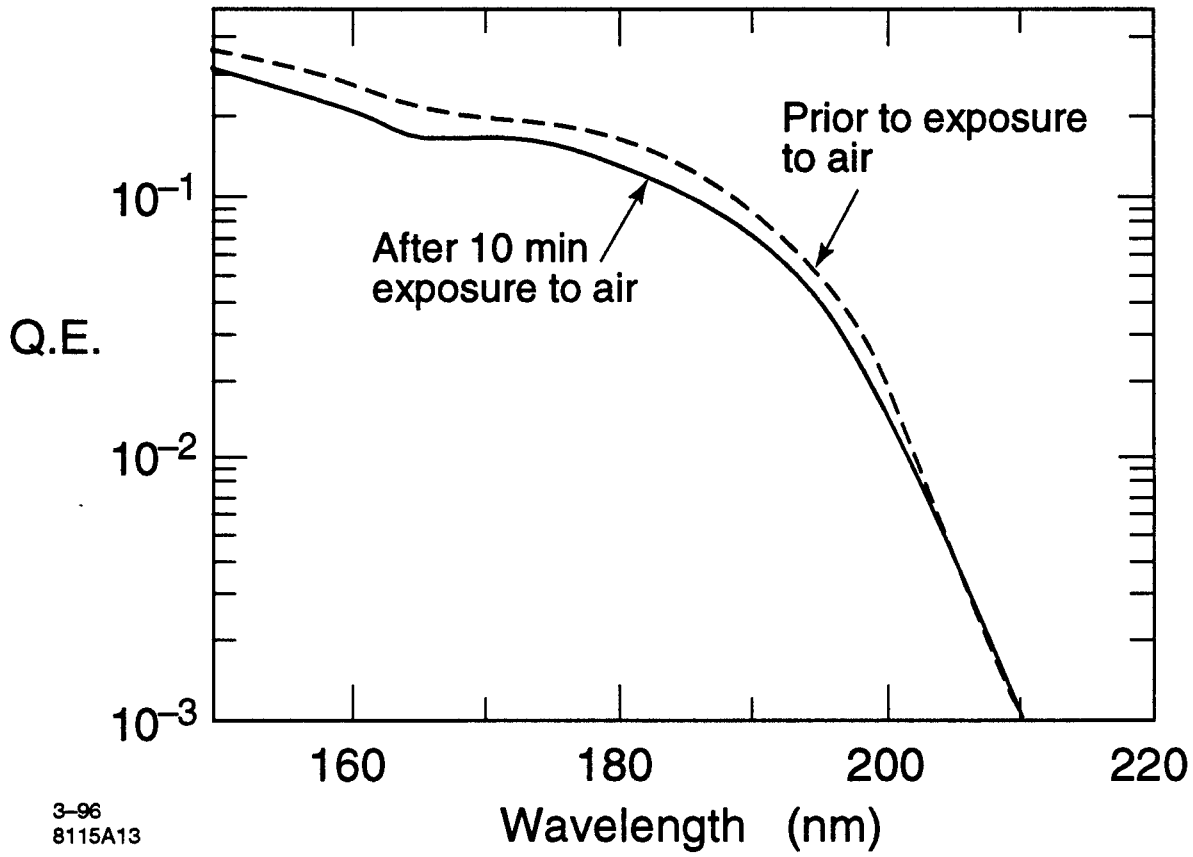
Prior to exposure
to air
After 10 min
exposure to air
Q.E.
10^{-1}
10^{-2}
10^{-3}
160
180
200
220
Wavelength (nm)
3-96
8115A13

Fig. 13

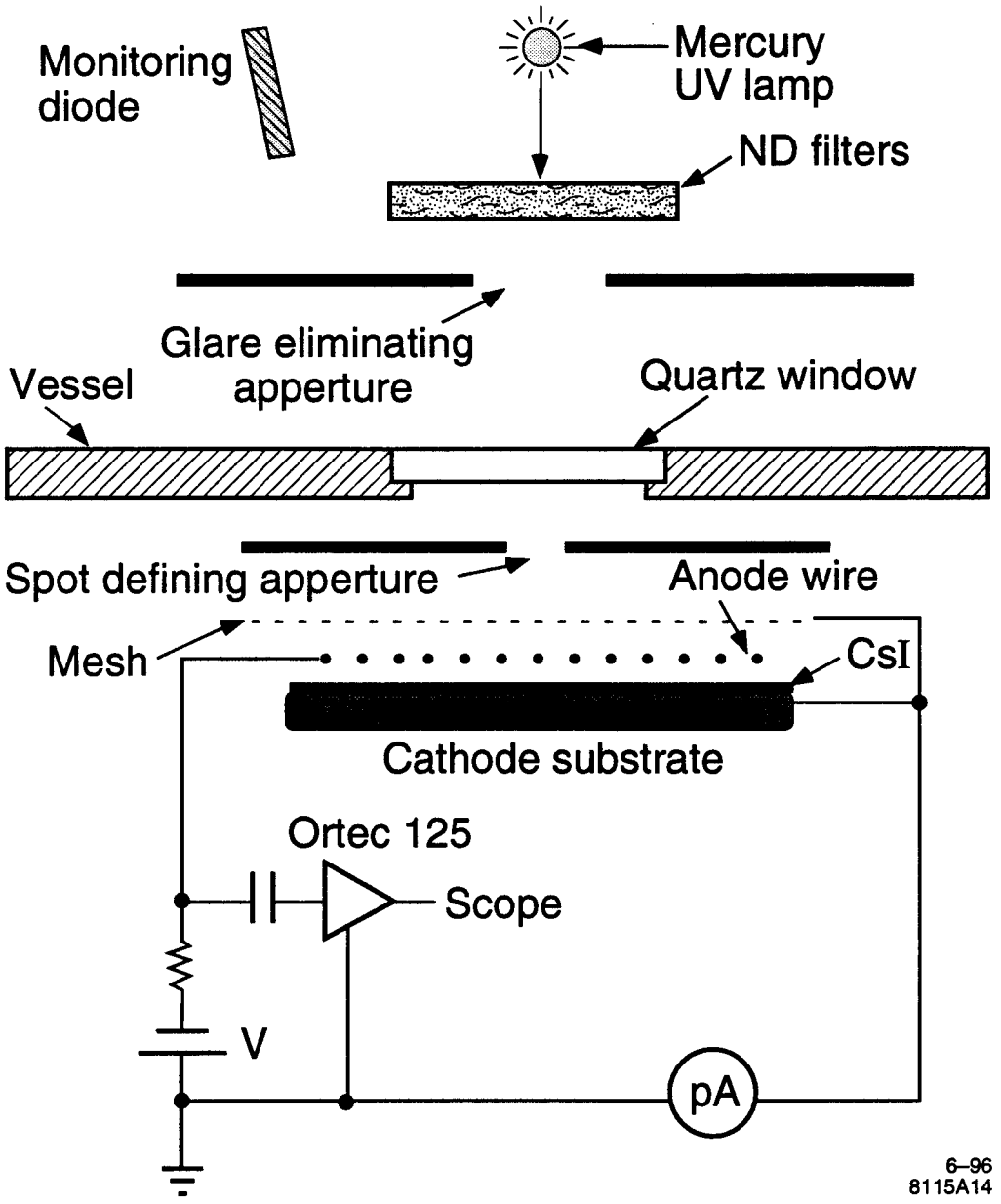
Monitoring diode
Mercury UV lamp
ND filters
Glare eliminating apperture
Vessel
Quartz window
Spot defining apperture
Anode wire
Mesh
CsI
Cathode substrate
Ortec 125
Scope
V
pA
6–96
8115A14

Fig. 14

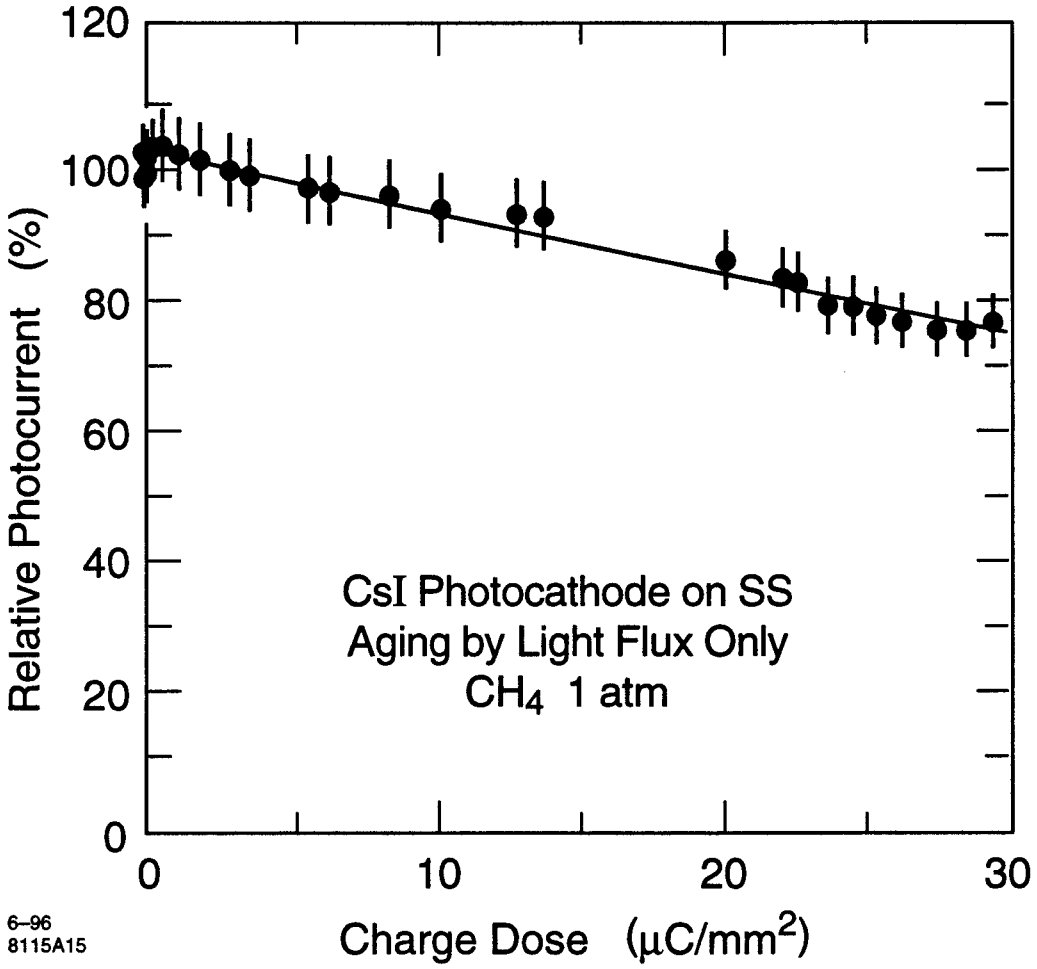
120
100
80
60
40
20
0
Relative Photocurrent (%)
CsI Photocathode on SS
Aging by Light Flux Only
CH_4 1 atm
0
10
20
30
Charge Dose ($\mu C/mm^2$)
6-96
8115A15

Fig. 15

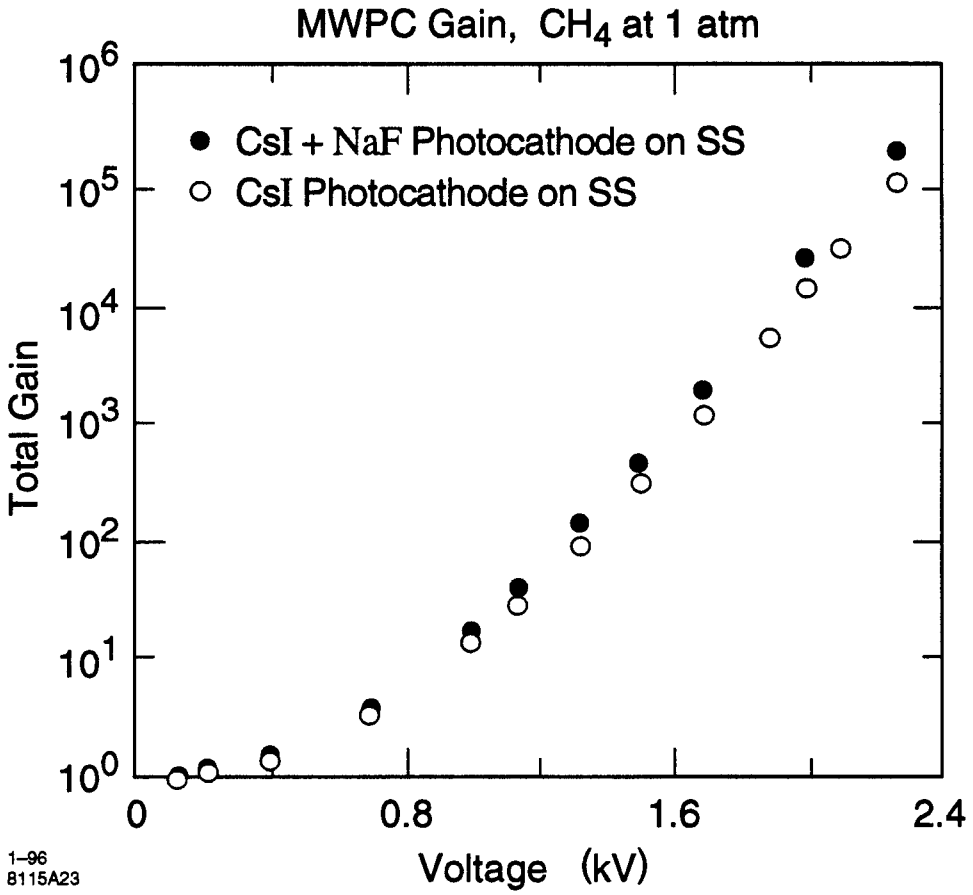
MWPC Gain, CH_4 at 1 atm
CsI + NaF Photocathode on SS
CsI Photocathode on SS
Total Gain
10^6
10^5
10^4
10^3
10^2
10^1
10^0
0
0.8
1.6
2.4
Voltage (kV)
1–96
8115A23

Fig. 16

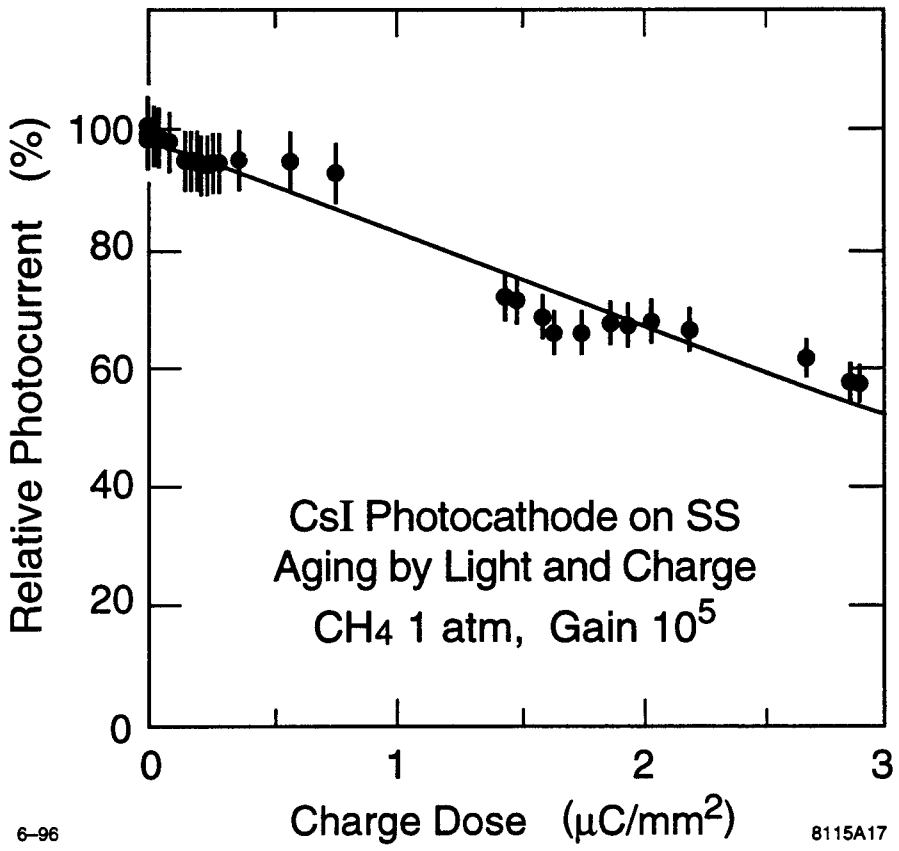
Relative Photocurrent (%)
100
80
60
40
20
0
0
1
2
3
Charge Dose (μC/mm²)
CsI Photocathode on SS
Aging by Light and Charge
CH4 1 atm, Gain 10⁵
6-96
8115A17

Fig. 17

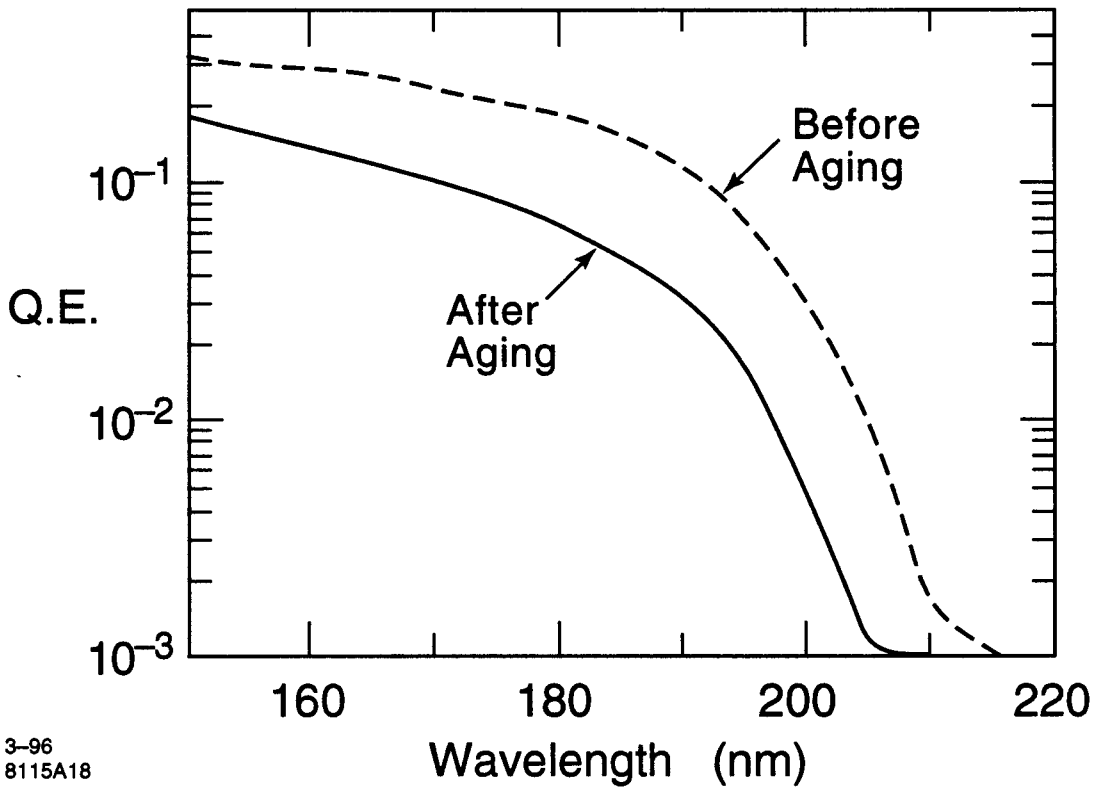
Before
Aging
After
Aging
Q.E.
10^{-1}
10^{-2}
10^{-3}
160
180
200
220
Wavelength (nm)
3-96
8115A18

Fig. 18

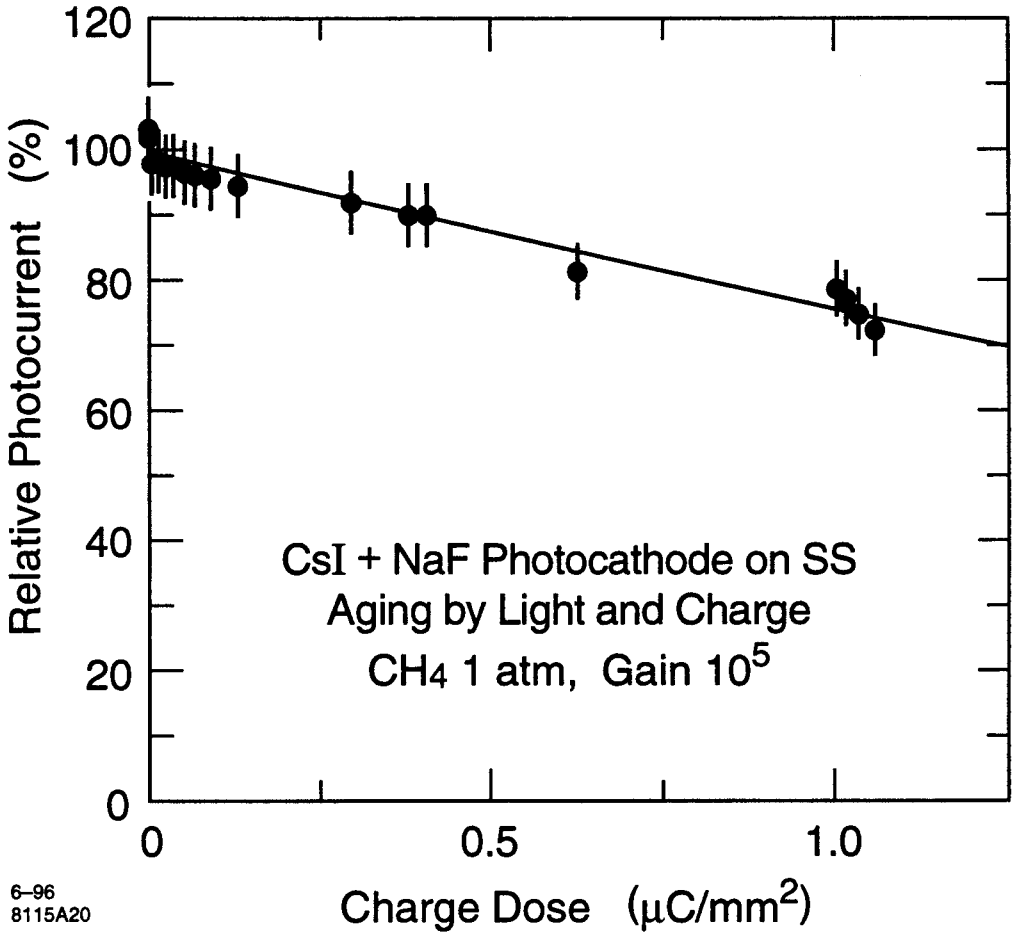
120
100
80
60
40
20
0
Relative Photocurrent (%)
CsI + NaF Photocathode on SS
Aging by Light and Charge
CH4 1 atm, Gain 10^5
0
0.5
1.0
Charge Dose (μC/mm^2)
6-96
8115A20

Fig. 19

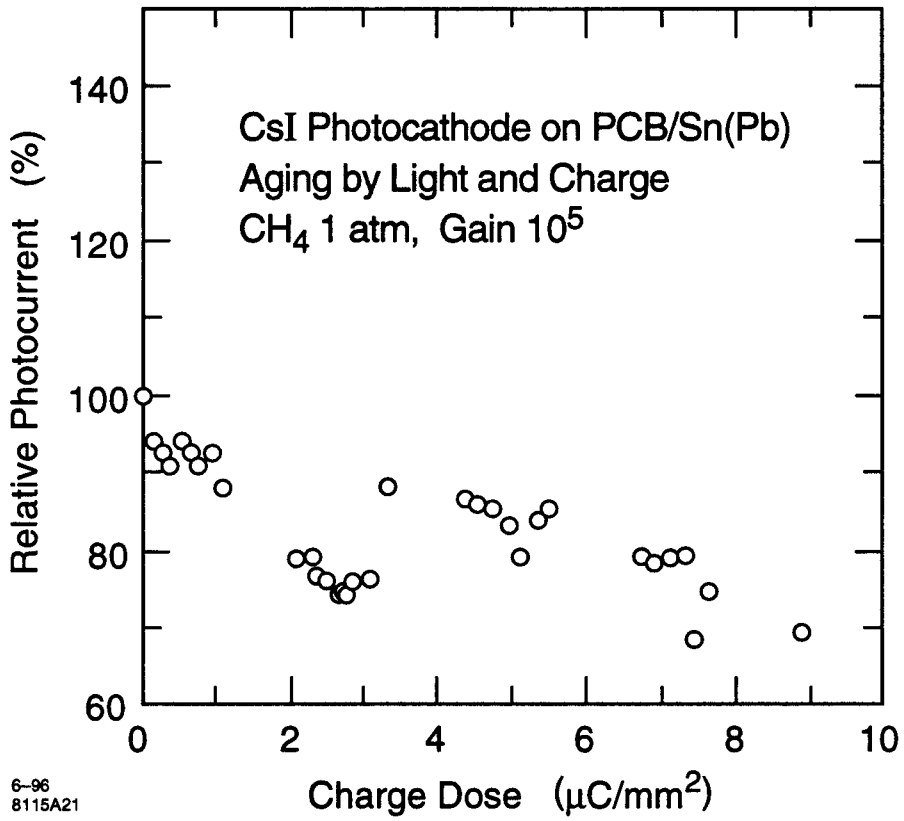
CsI Photocathode on PCB/Sn(Pb)
Aging by Light and Charge
CH_4 1 atm, Gain 10^5
Relative Photocurrent (%)
140
120
100
80
60
0
2
4
6
8
10
Charge Dose ($\mu C/mm^2$)
6-96
8115A21

Fig. 20

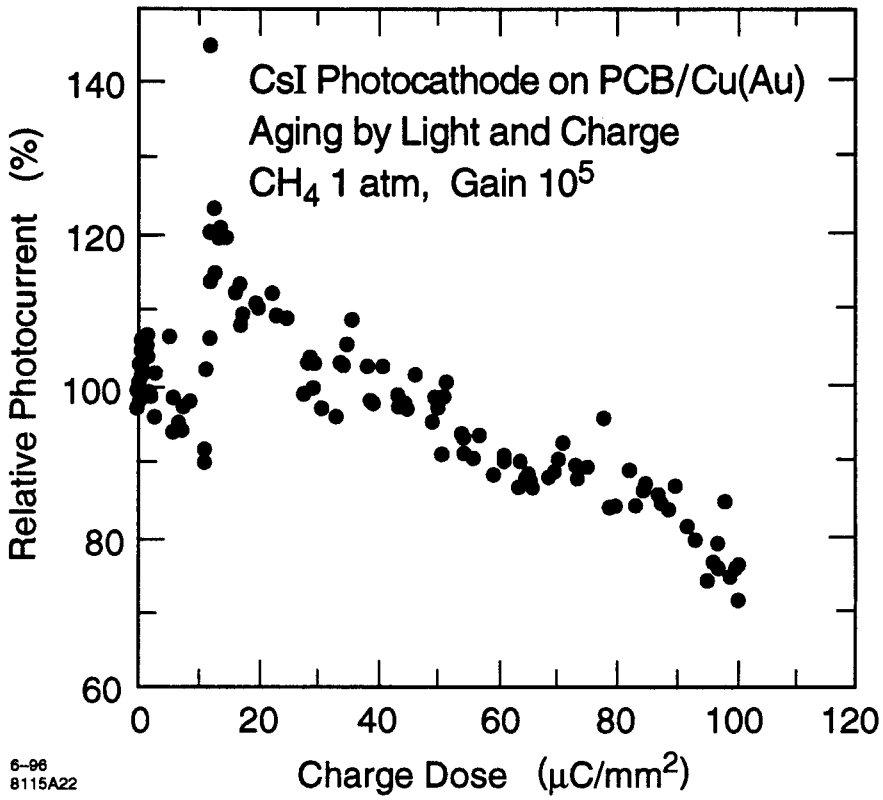
CsI Photocathode on PCB/Cu(Au)
Aging by Light and Charge
CH_4 1 atm, Gain 10^5
Relative Photocurrent (%)
140
120
100
80
60
0
20
40
60
80
100
120
Charge Dose (μC/mm²)
6-96
8115A22

Fg. 21